

Energy spectrum and wave-functions of four-dimensional
Supersymmetric Yang-Mills Quantum Mechanics for very
high cut-offs

Jan Koteński

M. Smoluchowski Institute of Physics, Jagellonian University
Reymonta 4, 30-059 Kraków, Poland

The spectrum of Supersymmetric Yang-Mills Quantum Mechanics (SYMQM) in $D=4$ dimensions for $SU(2)$ gauge group is computed for a maximal number of bosonic quanta $B \leq 60$ in the two-fermion sector with the angular momentum $j = 0$. We analyse the eigenfunctions of discrete and continuous spectra, test the scaling relation for the continuous spectrum and confirm the dispersion relation to high accuracy.

PACS numbers: 11.10.Kk, 04.60.Kz

Keywords: M-theory, SYMQM, spectrum, eigenfunctions, scaling

TPJU-08/2006

1. Introduction and summary of known results

In this work we consider Supersymmetric Yang-Mills Quantum Mechanics (SYMQM) [1, 2], which in $D = 10$ dimensions and for $SU(N \rightarrow \infty)$ gauge group according to the remarkable hypothesis [3, 4, 5] is equivalent to M -theory of $D0$ branes. Despite the fact that the three loop calculations [6, 5] question the exact equivalence, the SYMQM models possess a lot of fascinating properties required in M -theory, *i.e.* continuous spectrum of scattering states with the threshold states describing a supergraviton [7].

The SYMQM emerges from the dimensional reduction of supersymmetric Yang-Mills field theory in the $D - 1$ dimensional space to the effective Quantum Mechanics of zero momentum modes in a single point [2, 8]. In a gluinoless sector the energy spectrum of these system is identical to the spectrum of 0-volume glueballs [9, 10, 11, 12]. Although the resulting models are much simpler than the original field theories, they are rather complex with non-trivial solutions. Researches on the systems with $D < 10$ for various gauge groups provide the global understanding of whole family. Thus, the SYMQM provides a simple laboratory to study many properties of supersymmetric systems [2, 8]. For $D = 2$ and $SU(2)$ gauge group the system is exactly solvable. Going further to $D = 4$ dimensions the model becomes non-trivial. It possesses both localized and non-localized states.

The simplest method of solving the energy eigenproblem for the $D = 4$ model with $SU(2)$ group was introduced in Refs. [12, 13]. According to this method acting with bosonic and fermionic creation operators on the empty state one can construct a basis of Fock space. Next, in order to find the spectrum and the eigenfunctions of the Hamiltonian one can solve the eigenproblem of the Hamiltonian matrix calculated in the constructed basis. Since we have an infinite number of the states in the Fock space in order to perform numerical calculation we have to cut some basis vectors off. Therefore, in the above method one considers only Fock states with a number of bosonic quanta n_B smaller or equal to cut-off B . At the end making analysis of the spectrum as a function of cut-off B we are able to find the energy for the model without a cut-off. It turns out that due to commutativity properties between the Hamiltonian and the operator of number of fermionic quanta, n_F , the system separates into sectors with determined $n_F = 0, 1, \dots, 6$. Thus, we can solve the eigenproblem in smaller Fock basis with fixed n_F . The above method allowed to calculate the spectrum in all fermionic sectors with an arbitrary angular momentum j for the cut-off $B = 8$ and the Witten index for the model [12, 13].

It turns out that the Hamiltonian also commutes with an operator of the angular momentum j . This makes possible to construct the basis with fixed both n_F and the angular momentum, j . It was done by van Baal in

Refs. [14, 15] for $n_F = 0, 2, 4, 6$ and $j = 0$ but with the cut-off $B = 39$. Calculations for other sectors are more complicated within this approach.

The aim of this work is to analyse the spectrum of the $D = 4$ model with $SU(2)$ gauge group more precisely by enlarging cut-off yet further. Using the van Baal's method we concentrate on the sector with $F = 2$ and $j = 0$ where the supersymmetric vacuum state appears to be [15]. In this sector the eigenvalues of the Hamiltonian form discrete as well as continuous spectrum [16, 17]. For high cut-offs the wave-functions of discrete states converge with B and therefore we are able to build these eigenstates and describe properties of their wave-functions. Moreover, we can test the scaling properties [18] appearing for the continuous spectrum.

In the beginning of the next section we introduce a notation following Ref. [15] and describe the SYMQM model and show how one can construct Fock space in the $F = 2$ and $j = 0$ sector and calculate the Hamiltonian matrix. We also present the construction of the eigenstates of the Hamiltonian. Next we show the results which include the energy spectrum of the model for cut-off $B \leq 60$. Moreover, we construct and describe properties of the eigenfunctions for the discrete and continuous spectrum. At the end we confirm the scaling relation for the continuous spectrum which was derived in Ref. [18] for the cut free-particle and only conjectured for interaction systems.

2. Hamiltonian eigenproblem

2.1. Definitions

Following Refs. [9, 15] the supersymmetric Hamiltonian of Yang-Mills quantum mechanics with the $SU(2)$ gauge group has a form

$$H\delta_{\alpha\beta} = \frac{1}{2}\{Q_\alpha, Q_\beta^\dagger\}, \quad (2.1)$$

where Q and Q^\dagger are the generators of SUSY in the coordinate representation of the field theory defined as

$$Q_\alpha = \sigma_{\alpha\beta}^j \bar{\lambda}_a^{\dot{\beta}} \left(-i \frac{\partial}{\partial V_a^j} - i B_j^a \right) \quad \bar{Q}_{\dot{\alpha}} = \lambda_a^\beta \sigma_{\beta\dot{\alpha}}^j \left(-i \frac{\partial}{\partial V_a^j} + i B_j^a \right), \quad (2.2)$$

with Pauli matrices $\sigma^j = \tau^j$ and Weyl spinors λ_a^β . Here, a *colour magnetic* field of $SU(2)$ is defined as

$$B_i^a = -\frac{1}{2} g \varepsilon_{ijk} \varepsilon_{abc} V_j^b V_k^c, \quad (2.3)$$

where V_j^c are bosonic variables with colour indices $c = 1, 2, 3$ and spatial indices $j = 1, 2, 3$. The Weyl spinors λ_a^β with $\beta = 1, 2$ spinor indices and $a = 1, 2, 3$ colour indices satisfy the following anti-commutation relations

$$\{\lambda^{a\alpha}, \bar{\lambda}^{b\dot{\beta}}\} = \bar{\sigma}_0^{\dot{\beta}\alpha} \delta^{ab}, \quad \{\lambda^{a\alpha}, \lambda^{b\beta}\} = 0, \quad \{\bar{\lambda}^{a\dot{\alpha}}, \bar{\lambda}^{b\dot{\beta}}\} = 0, \quad (2.4)$$

where σ^0 is the unit matrix.

The SUSY generators satisfy

$$\{Q_\alpha, \bar{Q}_{\dot{\alpha}}\} = 2(\sigma_0)_{\alpha\dot{\alpha}} \mathcal{H} - 2(\sigma^i)_{\alpha\dot{\alpha}} V_i^a \mathcal{G}_a, \quad (2.5)$$

where

$$\mathcal{G}_a = ig\varepsilon_{abc} \left(V_j^c \frac{\partial}{\partial V_j^b} - \bar{\lambda}^b \bar{\sigma}_0 \lambda^c \right), \quad (2.6)$$

is the generator of the $SU(2)$ gauge transformation while the Hamiltonian density [8] is defined by

$$\mathcal{H} = -\frac{1}{2} \frac{\partial^2}{\partial V_i^a \partial V_i^a} + \frac{1}{2} B_i^a B_i^a - ig\varepsilon_{abc} \bar{\lambda}^a \bar{\sigma}^j \lambda^b V_j^c. \quad (2.7)$$

One may rescale bosonic variables V_i^a introducing new variables \hat{c}_i^a :

$$V_i^a = \frac{1}{g^{1/3}(L)L} \hat{c}_i^a. \quad (2.8)$$

Thus, performing the approximation of constant fields with $g(L \rightarrow 0) \rightarrow 0$ [9] with $g = g(L)L^3$ we obtain a Hamiltonian H independent of the coupling constant g :

$$\int d^3x \mathcal{H} \equiv g^{2/3}(L)H/L, \quad (2.9)$$

where

$$H = H_B + H_F, \quad (2.10)$$

with the bosonic part

$$H_B = -\frac{1}{2} \left(\frac{\partial}{\partial \hat{c}_i^a} \right)^2 + \frac{1}{2} \left(\hat{B}_i^a \right)^2, \quad (2.11)$$

and the fermionic one

$$H_F = -i\varepsilon_{abd} \bar{\lambda}^a \bar{\sigma}^i \lambda^b \hat{c}_i^d. \quad (2.12)$$

Here, the *colour magnetic* field is rescaled to

$$\hat{B}_i^a = -\frac{1}{2} \varepsilon_{ijk} \varepsilon_{abd} \hat{c}_j^b \hat{c}_k^d. \quad (2.13)$$

2.2. A straightforward approach

In this model there are 6 fermionic degrees of freedom, λ_a^β . An operator which gives the number of fermions, n_F , commutes with the Hamiltonian (2.10). Thus, our system splits into 7 sectors enumerated by n_F values. Since the sectors are related by a particle-hole symmetry

$$n_F \leftrightarrow 6 - n_F, \quad (2.14)$$

we have four independent sectors described by $n_F = 0, 1, 2, 3$.

In order to solve the eigenequation of the Hamiltonian (2.10) we construct an infinite basis of the Fock space by acting with \hat{c}_k^d and $\bar{\lambda}_k^{\dot{\alpha}}$ on the empty state:

$$|n\rangle = \sum_{\substack{\text{contractions} \\ \{a_1, \dots, a_r\}}} \hat{c}_{k_1}^{a_1} \dots \hat{c}_{k_m}^{a_m} \bar{\lambda}_{a_{m+1}}^{\dot{\alpha}} \dots \bar{\lambda}_{a_r}^{\dot{\beta}} |0\rangle, \quad (2.15)$$

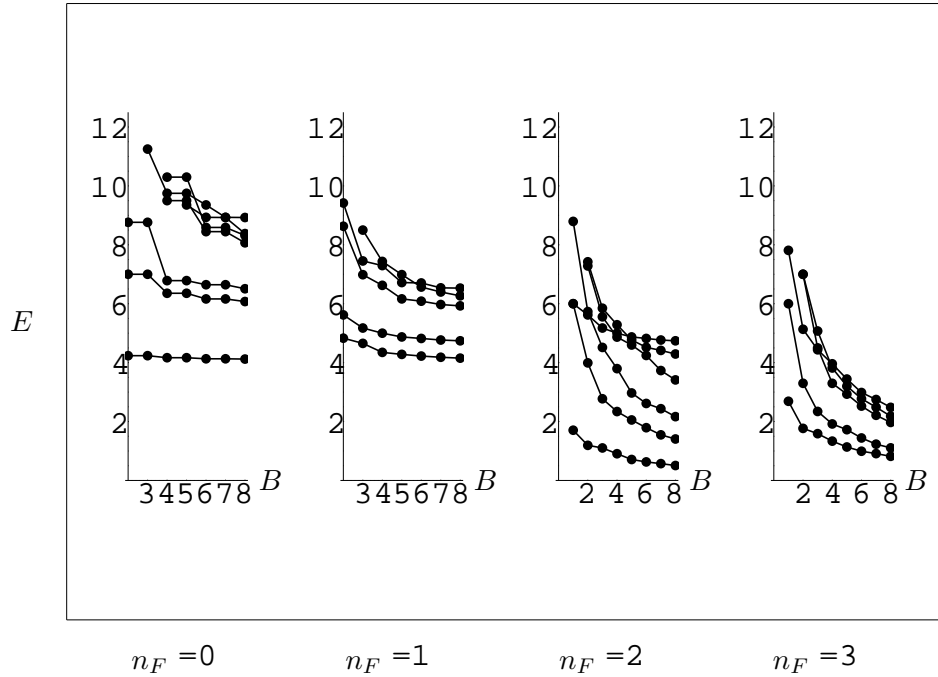
where \hat{c}_k^d and $\bar{\lambda}_k^{\dot{\alpha}}$ are given by appropriate linear combinations of the creation and annihilation bosonic and fermionic operators, respectively, while the sum goes over gauge invariant linear combinations of \hat{c}_k^d and $\bar{\lambda}_k^{\dot{\alpha}}$, [12]¹. Next, we act with (2.10) on the basis states (2.15) calculating matrix elements of the Hamiltonian. Finally, we diagonalize the Hamiltonian matrix finding eigenvalues and eigenstates of (2.10).

Contrary to fermions we have an infinite number of bosons, $n_B = 0, \dots, \infty$. Moreover, the operator which describes a number of bosons n_B does not commute with the Hamiltonian (2.10). Therefore, our Hamiltonian matrix is infinite. To simplify the problem we cut the basis (2.15) by considering only the states with $n_B \leq B$, where B is defined as a cut-off. Next, analysing the limit $B \rightarrow \infty$ we recover the spectrum of the full, infinite Hamiltonian matrix.

Eigenstates of the model are linear combinations of basis states (2.15). It turns out that for given n_B we have a large number of states. Even if we divide the problem into the separate fermionic sectors, the separate bases have large numbers of states. One can see it in Table 1 from Ref. [13] where the authors show the size of the basis containing states generated in specified fermionic sectors labelled by n_F and for given n_B . In this Table N_s describes a number of basis vectors with a given bosonic quantum numbers whereas Σ is a sum of vectors in the basis with maximal quantum number n_B . The last column shows that the number of bosonic states $\Sigma_B = \Sigma_0 + \Sigma_2 + \Sigma_4 + \Sigma_6$ is equal to the number of fermionic states $\Sigma_F = \Sigma_1 + \Sigma_3 + \Sigma_5$ as required by supersymmetry.

¹ Here, calculations are performed in Fock-space representation

n_F	0		1		2		3		
n_B	N_s	Σ_0	N_s	Σ_1	N_s	Σ_2	N_s	Σ_3	$\Sigma_B - \Sigma_F$
0	1	1	-	-	1	1	4	4	0
1	-	1	6	6	9	10	6	10	0
2	6	7	6	12	21	31	42	52	0
3	1	8	36	48	63	94	56	108	0
4	21	29	36	84	111	205	192	300	0
5	6	35	126	210	240	445	240	540	0
6	56	91	126	336	370	815	600	1140	0
7	21	112	336	672	675	1490	720	1860	0
8	126	238	336	1008	960	2450	1500	3360	0
j_{\max}	8		17/2		9		19/2		

Table 1. Size of the basis generated in specified fermionic sectors n_F from Ref. [13]Figure 1. Dependence of the energy E on a cut-off $B \geq n_B$ in sectors with various n_F obtained in Ref. [13]

In Fig. 1 we present a dependence of the energy on the cut-off. One can see that for this large number of bosonic quanta the energy converges to

the constant value rather slowly, especially for $n_F = 2, 3, 4$. Thus, in order to simplify this problem, we find another operator which commutes with the Hamiltonian, *i.e.* the total angular momentum j . Using the operator describing a fermion number, n_F , and the total angular momentum, we can divide the spectrum into smaller sectors labelled by n_F and j . This will be discussed below.

2.3. Analytic change of variables

In the rest of the paper we consider the case with $n_F = 2$ and $j = 0$. This case is most interesting because it contains the vacuum state of the system. Moreover, the energy has discrete and continuous spectrum. We will use the notation following the work of van Baal [15, 14].

The gauge invariance and the vanishing angular momentum j allow us to reduce a number of bosonic variables [15]. The reduction can be rewritten as a diagonalization of \hat{c}_i^a :

$$\hat{c}_i^a = \sum_{j=1}^3 R_{ij} x_j T^{ja}, \quad (2.16)$$

where matrices $R, T \in SO(3)$. Thus, from nine bosonic variables \hat{c}_i^a one obtains three invariants of both gauge and rotation groups:

$$-\infty < x_i < \infty, \quad \text{where } i = 1, 2, 3. \quad (2.17)$$

Additionally, the second set of invariant variables (r, u, v) is introduced where

$$r^2 = (\hat{c}_j^a)^2 = \sum_{j=1}^3 x_j^2, \quad (2.18)$$

defines the radius r in the $\{x_j\}$ -space, so that $0 \leq r \leq \infty$, while

$$u = r^{-4} (\hat{B}_j^a)^2 = r^{-4} \sum_{i>j=1}^3 x_i^2 x_j^2, \quad (2.19)$$

takes values $0 \leq u \leq \frac{1}{3}$ and corresponds to the rescaled bosonic potential

$$V(\vec{x}) = x_1^2 x_2^2 + x_1^2 x_3^2 + x_2^2 x_3^2 = u r^4. \quad (2.20)$$

An example of equipotential surface is shown in Fig. 2. The potential has minimum on x_i -axes. Due to the rescaling property (2.20) of $V(\vec{x})$ all equipotential surfaces with different values of energy have the same shape.

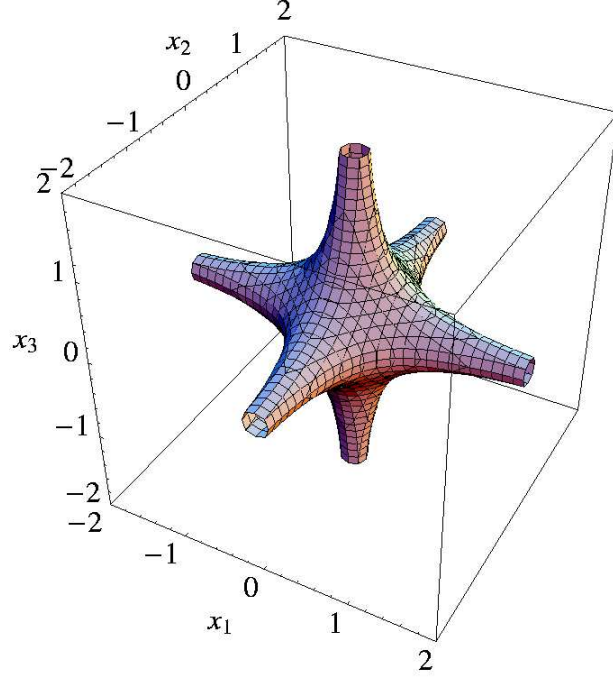


Figure 2. An example of equipotential surface for $V(\vec{x}) = ur^4 = x_1^2 x_2^2 + x_1^2 x_3^2 + x_2^2 x_3^2 = 0.1$

It turns out that for $n_F = 2$ the fermionic part of the Hamiltonian breaks the symmetry

$$x_1 x_2 x_3 \leftrightarrow -x_1 x_2 x_3. \quad (2.21)$$

Thus, in order to describe the system completely one has to introduce the remaining variable

$$v = r^{-3} \det \hat{c} = r^{-3} \prod_{j=1}^3 x_j, \quad (2.22)$$

which may take positive as well as negative values $-1/\sqrt{27} \leq v \leq 1/\sqrt{27}$.

One can notice that the transition from (r, u, v) to (x_1, x_2, x_3) is not unique. The transformation functions $x_j(r, u, v)$ between coordinates are 24-valued functions and we can choose one branch, *i.e.* imposing $|x_1| \leq x_2 \leq x_3$. It turns out that for $n_F = 2$ and $j = 0$ bosonic terms of our calculations can be rewritten in (x_1, x_2, x_3) variables or equivalently in (r, u, v) coordinates. After integrating out six angular variables, the integral measure changes into

$$d^9 \hat{c} = \frac{2}{3} \pi^4 J d^3 x, \quad (2.23)$$

with the Jacobian J defined as

$$J \equiv \prod_{i>j} |x_i^2 - x_j^2| = r^6 \sqrt{u^2(1-4u) - v^2(4-18u+27v^2)}. \quad (2.24)$$

Let us consider the basis vectors (2.15). For $n_F = 2$ they contain two fermionic creation operators $\bar{\lambda}_\alpha^a$. We can form either antisymmetric

$$|\mathcal{V}\rangle \equiv \mathcal{V}_j^c \mathcal{I}_c^j = -2i \mathcal{V}_j^c \varepsilon_{abc} \bar{\lambda}_\alpha^a (\bar{\sigma}^{j0})^{\dot{\alpha}\beta} \bar{\lambda}^{b\dot{\beta}} |0\rangle, \quad (2.25)$$

or symmetric

$$|\mathcal{S}\rangle \equiv \mathcal{S}_{ab} \mathcal{J}^{ab} = -\mathcal{S}_{ab} \bar{\lambda}_\alpha^a \bar{\lambda}_\beta^b \epsilon^{\dot{\alpha}\dot{\beta}} |0\rangle, \quad (2.26)$$

combinations, where \mathcal{V}_j^c and \mathcal{S}_{ab} are antisymmetric and symmetric combinations of bosonic variables \hat{c}_j^a respectively, while $\bar{\sigma}^{j0}$ is related to Pauli matrices by $\bar{\sigma}^{j0} = \frac{1}{2}\tau_j$. The covariance gives us their structure as

$$\mathcal{V}_j^a = h_1(r, u, v) \hat{c}_j^a / r - h_2(r, u, v) \hat{B}_j^a / r^2 + h_3(r, u, v) \hat{c}_j^b \hat{c}_k^b \hat{c}_k^a / r^3, \quad (2.27)$$

and

$$\mathcal{S}^{ab} = h_4(r, u, v) \delta^{ab} - h_5(r, u, v) \hat{c}_j^a \hat{c}_j^b / r^2 + h_6(r, u, v) \hat{c}_j^b \hat{c}_j^d \hat{c}_k^d \hat{c}_k^b / r^4, \quad (2.28)$$

where $h_i(r, u, v)$ are functions of invariant variables. Finally, our basis vector may have both invariant parts, so that

$$|\Psi\rangle = |\mathcal{V}\rangle + |\mathcal{S}\rangle. \quad (2.29)$$

The Eqs. (2.27)-(2.29) can be rewritten as

$$|\Psi\rangle = \sum_{\mu=1}^6 h_\mu(r, u, v) |e_\mu(u, v)\rangle, \quad (2.30)$$

where

$$\begin{aligned} |e_1(u, v)\rangle &= \hat{c}_j^a / r \mathcal{I}_a^j, & |e_4(u, v)\rangle &= \delta^{ab} \mathcal{J}_{ab}, \\ |e_2(u, v)\rangle &= \hat{B}_j^a / r^2 \mathcal{I}_a^j, & |e_5(u, v)\rangle &= \hat{c}_j^a \hat{c}_j^b / r^2 \mathcal{J}_{ab}, \\ |e_3(u, v)\rangle &= \hat{c}_j^b \hat{c}_k^b \hat{c}_k^a / r^3 \mathcal{I}_a^j, & |e_6(u, v)\rangle &= \hat{c}_j^b \hat{c}_j^d \hat{c}_k^d \hat{c}_k^b / r^4 \mathcal{J}_{ab}. \end{aligned} \quad (2.31)$$

Lowering of indices can be done with $\epsilon_{\alpha\beta} = \epsilon_{\dot{\alpha}\dot{\beta}} = -i\tau_2$ for spinor indices, δ_{ab} for colour group indices and δ_{ij} for space indices. Now, we are ready to reformulate our Hamiltonian (2.10) in terms of (r, u, v) .

The fermionic part of H_F can be expanded in the space spanned by $|e_\mu\rangle \equiv |e_\mu(u, v)\rangle$, *i.e.*

$$H_F|e_\mu\rangle = \sum_{\nu=1}^6 |e_\nu\rangle H_F^{\nu\mu}, \quad (2.32)$$

which gives a 6×6 matrix in a form

$$H_F^{\mu\nu}/r = \begin{pmatrix} 0 & 1 & -v & 2 & 1 & 1-u \\ 2 & 0 & 1 & 0 & 0 & -v \\ 0 & -1 & 0 & 0 & -1 & -1 \\ 2 & 4v & 2-4u & 0 & 0 & 0 \\ -2 & 0 & 0 & 0 & 0 & 0 \\ 0 & 0 & -2 & 0 & 0 & 0 \end{pmatrix}. \quad (2.33)$$

The vectors $|e_\mu(u, v)\rangle$ are not orthogonal and their scalar products² can be written in a matrix form as

$$N^{\mu\nu} = \langle e_\mu | e_\nu \rangle_F = \begin{pmatrix} 8 & 24v & 8X & 0 & 0 & 0 \\ 24v & 8u & 8v & 0 & 0 & 0 \\ 8X & 8v & 8Y & 0 & 0 & 0 \\ 0 & 0 & 0 & 12 & 4 & 4X \\ 0 & 0 & 0 & 4 & 4X & 4Y \\ 0 & 0 & 0 & 4X & 4Y & 4Z \end{pmatrix}, \quad (2.34)$$

where

$$X = 1 - 2u, \quad Y = 1 - 3u + 3v^2 \quad \text{and} \quad Z = 1 + 2u^2 - 4u + 4v^2. \quad (2.35)$$

Thus, calculating scalar products of the states (2.30) we have to use the $N^{\nu\mu}$ matrix, *i.e.*

$$\langle \Psi | \Psi' \rangle = \int d^9 \hat{c} \sum_{\mu, \nu=1}^6 h_\mu^* N^{\mu\nu} h'_\nu, \quad (2.36)$$

with h_ν defined in (2.27)-(2.28). Similarly, the matrix elements have a form

$$\langle \Psi | H | \Psi' \rangle = \int d^9 \hat{c} \sum_{\mu, \nu, \rho=1}^6 h_\mu^* N^{\mu\nu} H^{\nu\rho} h'_\rho. \quad (2.37)$$

The kinetic part of the Hamiltonian (2.10) is given by

$$-\frac{1}{2} \frac{\partial^2}{(\partial \hat{c}_i^a)^2} = -\frac{1}{2} J^{-1}(\vec{x}) \frac{\partial}{\partial x_j} J(\vec{x}) \frac{\partial}{\partial x_j} = -\frac{1}{2} \left(r^{-8} \frac{\partial}{\partial r} r^8 \frac{\partial}{\partial r} + \frac{\Delta(u, v)}{r^2} \right), \quad (2.38)$$

² These scalar products, *i.e.* $\langle \cdot | \cdot \rangle_F$, are performed with integration only over fermionic degrees of freedom

where the Laplacian on a 9-dimensional sphere reads

$$\begin{aligned} \Delta(u, v) = & 4(3v^2 + u - 4u^2) \frac{\partial^2}{(\partial u)^2} + 8(1 - 3u)v \frac{\partial^2}{\partial u \partial v} + (u - 9v^2) \frac{\partial^2}{(\partial v)^2} \\ & + 4(2 - 11u) \frac{\partial}{\partial u} - 30v \frac{\partial}{\partial v}. \end{aligned} \quad (2.39)$$

Similarly to (2.32), the matrix elements of $\Delta(u, v)$ can be calculated as

$$-\frac{1}{2} \Delta(u, v) \sum_{\mu=1}^6 h_{\mu}(r, u, v) |e_{\mu}(u, v)\rangle = \sum_{\mu, \nu=1}^6 |e_{\nu}(u, v)\rangle \hat{H}_{\Delta}^{\nu\mu} h_{\mu}(r, u, v), \quad (2.40)$$

where $\hat{H}_{\Delta}^{\nu\mu}$ is found in Ref. [15] as

$$\hat{H}_{\Delta}^{\mu\nu} = -\frac{1}{2} \delta^{\mu\nu} \Delta(u, v) - \frac{1}{2} \begin{pmatrix} \Delta_{\mathcal{V}}^1 & \emptyset \\ \emptyset & \Delta_{\mathcal{S}}^1 \end{pmatrix} - \frac{1}{2} \begin{pmatrix} \Delta_{\mathcal{V}}^0 & \emptyset \\ \emptyset & \Delta_{\mathcal{S}}^0 \end{pmatrix}, \quad (2.41)$$

with

$$\Delta_{\mathcal{V}}^1 \equiv 2 \begin{pmatrix} (2 - 4u)\partial_u - 3v\partial_v & \partial_v + 2v\partial_u & 3v\partial_v + 6u\partial_u \\ \partial_v & (2 - 8u)\partial_u - 6v\partial_v & -6v\partial_u \\ -2\partial_u & -\partial_v & -12u\partial_u - 9v\partial_v \end{pmatrix}, \quad (2.42)$$

$$\Delta_{\mathcal{S}}^1 \equiv 2 \begin{pmatrix} 0 & 2v\partial_v & -8v^2\partial_u \\ 0 & (4 - 8u)\partial_u - 6v\partial_v & 4v\partial_v + 8u\partial_u \\ 0 & -4\partial_u & -16u\partial_u - 12v\partial_v \end{pmatrix}, \quad (2.43)$$

and

$$\Delta_{\mathcal{V}}^0 \equiv 2 \begin{pmatrix} -4 & 0 & 7 \\ 0 & -9 & 0 \\ 0 & 0 & -15 \end{pmatrix}, \quad \Delta_{\mathcal{S}}^0 \equiv \begin{pmatrix} 0 & 3 & 1 \\ 0 & -9 & 11 \\ 0 & 0 & -22 \end{pmatrix}. \quad (2.44)$$

To sum up, we obtain the 6×6 Hamiltonian matrix in a form

$$\hat{H}^{\mu\nu} = -\frac{1}{2} \delta^{\mu\nu} r^{-8} \frac{\partial}{\partial r} r^8 \frac{\partial}{\partial r} + r^{-2} \hat{H}_{\Delta}^{\mu\nu} + \frac{1}{2} \delta^{\mu\nu} r^4 u + r \hat{H}_F^{\mu\nu}, \quad (2.45)$$

where $\hat{H}_F^{\mu\nu} = H_F^{\mu\nu}/r$.

2.4. The Fock space

Following Ref. [15] we choose the eigenvectors of the harmonic oscillator as the basis vectors (2.30). Substituting (r, u, v) variables these eigenfunctions separate into a spherical and radial part as follows³

$$|\hat{\Psi}^{(n,\ell,m)}(r, u, v)\rangle = \sum_{\mu=1}^6 h_{\mu}^{(n,\ell,m)}(r, u, v)|e_{\mu}\rangle, \quad (2.46)$$

with

$$h_{\mu}^{(n,\ell,m)}(r, u, v) = \mathcal{Y}_{\mu}^{(\ell,m)}(u, v)\phi_n^{\ell}(r). \quad (2.47)$$

Next, to orthonormalize the basis (2.46) the Gram-Schmidt process

$$|\hat{\Psi}^{(n,\ell,m)}(r, u, v)\rangle \xrightarrow{\text{ortonorm.}} |\Psi^{(n,\ell,m)}(r, u, v)\rangle, \quad (2.48)$$

is performed.

Construction of the spherical harmonics

$$\mathcal{Y}^{(\ell,m)} = \langle u, v|\ell, m\rangle = (\mathcal{Y}_1^{(\ell,m)}, \mathcal{Y}_2^{(\ell,m)}, \dots, \mathcal{Y}_6^{(\ell,m)}), \quad (2.49)$$

is shown in Ref. [15]. They satisfy the eigenequation

$$\hat{H}_{\Delta}\mathcal{Y}^{(\ell,m)} = L(2L + 7)\mathcal{Y}^{(\ell,m)}, \quad (2.50)$$

where the *angular momentum* $L = \frac{1}{2}(\ell - 3)$ is a half-integer number and its degeneration is described for *even* $2L$ by

$$m = 0, 1, 2, \dots, L, \quad (2.51)$$

and for *odd* $2L$ by

$$m = \frac{1}{2}, \frac{3}{2}, \dots, L. \quad (2.52)$$

A first few spherical harmonics are presented in Table 2. As we can see the spherical harmonics are six-component vectors of polynomials in u and v .

The radial part of the Schrödinger equation for the harmonic oscillator gives the eigenequation

$$\left[-\frac{1}{2}r^{-8}\partial_r r^8\partial_r + \frac{1}{2}\frac{(\ell+4)(\ell-3)}{r^2} + \frac{1}{2}r^2 \right] \phi_n^{\ell}(r) = \tilde{E}_n^{\ell}\phi_n^{\ell}(r). \quad (2.53)$$

³ In the following sections all sums will be written directly. There is no summation over repeating indices assumed a priori

$\frac{1}{2}(\ell - 3)$	m	$\mathcal{Y}^{(\ell,m)} = (\mathcal{Y}_1^{(\ell,m)}, \mathcal{Y}_2^{(\ell,m)}, \dots, \mathcal{Y}_6^{(\ell,m)})$
0	0	$(0, 0, 0, 1, 0, 0) \sqrt{35/2}/8\pi^2$
$\frac{1}{2}$	$\frac{1}{2}$	$(1, 0, 0, 0, 0, 0) \sqrt{105}/16\pi^2$
1	0	$(0, 1, 0, 0, 0, 0) \sqrt{1155/2}/16\pi^2$
1	1	$(0, 0, 0, -\frac{1}{3}, 1, 0) 3\sqrt{77}/16\pi^2$
$\frac{3}{2}$	$\frac{1}{2}$	$(0, 0, 0, v, 0, 0) \sqrt{15015}/16\pi^2$
$\frac{3}{2}$	$\frac{3}{2}$	$(-\frac{7}{11}, 0, 1, 0, 0, 0) 11\sqrt{273/5}/32\pi^2$
2	0	$(v, -\frac{1}{13}, 0, 0, 0, 0) 39\sqrt{77}/32\pi^2$
2	1	$(0, 0, 0, \frac{10}{143}, -\frac{11}{13}, 1) 429\sqrt{7/86}/16\pi^2$
2	2	$(0, 0, 0, -\frac{6}{43} + u, -\frac{22}{43}, \frac{26}{43}) 3\sqrt{6149/2}/16\pi^2$
$\frac{5}{2}$	$\frac{1}{2}$	$(0, 0, 0, -\frac{v}{3}, v, 0) 3\sqrt{51051/2}/16\pi^2$
$\frac{5}{2}$	$\frac{3}{2}$	$(-\frac{11}{195}, v, \frac{1}{15}, 0, 0, 0) 39\sqrt{1785}/64\pi^2$
$\frac{5}{2}$	$\frac{5}{2}$	$(-\frac{1}{4} + u, -\frac{13v}{44}, \frac{5}{44}, 0, 0, 0) 33\sqrt{221/7}/16\pi^2$
3	0	$(-\frac{10v}{17}, \frac{1}{51}, v, 0, 0, 0) 51\sqrt{4389/5}/32\pi^2$
3	1	$(-\frac{6v}{13}, -\frac{12}{65} + u, \frac{38v}{65}, 0, 0, 0) 39\sqrt{17765/7}/64\pi^2$
3	2	$(0, 0, 0, \frac{4}{663} - \frac{u}{17} + v^2, 0, 0) 663\sqrt{209/7}/32\pi^2$
3	3	$(0, 0, 0, \frac{2}{51} - \frac{3u}{17}, -\frac{6}{17} + u, \frac{4}{17}) 51\sqrt{2717/7}/32\pi^2$
$\frac{7}{2}$	$\frac{1}{2}$	$(0, 0, 0, \frac{28v}{323}, -\frac{15v}{19}, v) 969\sqrt{231/10}/32\pi^2$
$\frac{7}{2}$	$\frac{3}{2}$	$(0, 0, 0, -\frac{12v}{65} + uv, -\frac{6v}{13}, \frac{38v}{65}) 39\sqrt{53295/2}/32\pi^2$
$\frac{7}{2}$	$\frac{5}{2}$	$(\frac{10}{969} - \frac{u}{19} + v^2, -\frac{2v}{19}, -\frac{2}{323}, 0, 0, 0) 969\sqrt{429/14}/32\pi^2$
$\frac{7}{2}$	$\frac{7}{2}$	$(\frac{44}{399} - \frac{93u}{133} + \frac{2v^2}{7}, \frac{2v}{7}, -\frac{20}{133} + u, 0, 0, 0) 19\sqrt{51051/2}/64\pi^2$

Table 2. Orthonormal spherical harmonics for $L < 4$ from Ref. [15]

The solution to Eq. (2.53) has a form

$$\phi_n^\ell(r) = \sqrt{2n!} \frac{e^{-r^2/2} r^{\ell-3} L_n^{\ell+\frac{1}{2}}(r^2)}{\sqrt{\Gamma(n + \ell + \frac{3}{2})}}, \quad (2.54)$$

where $L_n^\ell(x)$ are Laguerre polynomials, while quantum numbers

$$n = 0, 1, 2, \dots, \infty, \quad (2.55)$$

and

$$\ell = 2L + 3 = 3, 4, 5, \dots, \infty, \quad (2.56)$$

enumerate different radial solutions. The oscillator energy defined by (2.53) is a function of the above quantum numbers:

$$\tilde{E}_n^\ell = \ell + 2n + \frac{3}{2}. \quad (2.57)$$

Since the number of degrees of freedom in the system is nine a number of bosonic quanta for a given basis vector (2.48) reads

$$n_B = \tilde{E}_n^\ell - \frac{9}{2} = \ell + 2n - 3. \quad (2.58)$$

The above formula will be used to relate the quantum numbers ℓ and n to the cut-off $B \geq n_B$.

Let us consider the integrals over (r, u, v) which appear in the scalar products of the wavefunctions, (2.36) and (2.37). Due to the simplicity of (r, u, v) variables and the polynomial form of the eigenstates \mathcal{Y}_n to (2.50), one can perform the integrals of the spherical harmonics over u and v :

$$X_{i,j} \equiv \int_{r=1} d^9 \hat{c} u^i v^{2j}, \quad (2.59)$$

by making use of the recurrence relation

$$X_{i,j} = \frac{4i(1+i+4j)X_{i-1,j} + 12i(i-1)X_{i-2,j+1} + 2j(2j-1)X_{i+1,j-1}}{(4i+6j)(4i+6j+7)}, \quad (2.60)$$

where $X_{0,0} = 32\pi^4/105$. Since the radial functions (2.54) are orthonormal using

$$\int dr r^8 \phi_n^\ell(r)^* \phi_{n'}^\ell(r) = \delta_{nn'}, \quad (2.61)$$

one can also easily perform the integrals over r .

2.5. Hamiltonian matrix and the eigenfunctions

In the last section we have shown the way to construct the Hamiltonian matrix of the SYMQM model for $D = 2$ and the $SU(2)$ group. Now, we are ready to construct the matrix elements and the eigenfunctions of the Hamiltonian in the cut Fock space (2.48). Thus, applying (2.37) and (2.59)-(2.61) we calculate matrix elements of (2.45) as

$$H^{(n',\ell',m'),(n,\ell,m)} = \langle n', \ell', m' | H | n, \ell, m \rangle, \quad (2.62)$$

where $|n, \ell, m\rangle \equiv |\Psi^{(n,\ell,m)}(r, u, v)\rangle$. Next, we solve the eigenequation

$$\sum_{(n,\ell,m)} H^{(n',\ell',m'),(n,\ell,m)} v_k^{(n,\ell,m)} = E_k v_k^{(n',\ell',m)}, \quad (2.63)$$

where the eigenvalues E_k describe the spectrum of the Hamiltonian (2.10)⁴. Finally, we find the eigenfunctions of (2.10) in the basis (2.48) as

$$\begin{aligned} |\Phi_k(r, u, v)\rangle &= \sum_{(n,\ell,m)} v_k^{(n,\ell,m)} |\Psi^{(n,\ell,m)}(r, u, v)\rangle = \\ &= \sum_{(n,\ell,m)} v_k^{(n,\ell,m)} \sum_{m=1}^6 \mathcal{Y}_\mu^{(\ell,m)}(u, v) \phi_n^\ell(r) |e_\mu\rangle, \end{aligned} \quad (2.64)$$

where $\mathcal{Y}_\mu^{(\ell,m)}(u, v)$ are spherical harmonics satisfying (2.50) while $\phi_n^\ell(r)$ are defined by (2.54). The non-orthogonal vectors $|e_\mu\rangle$ contain the fermionic variables and their scalar product is defined by (2.34). The above formula is the main expression which we use to compute the wave-functions of the model.

3. Results

3.1. Eigenenergies, coexistence and B -dependence

Solving the eigenequation (2.63) for different cut-off B we obtain the energy spectrum of the system with $j = 0$ and $n_F = 2$ as a function of B . Using Alpha DEC, PC computers and optimized C++ code we were able to reach the cut-off values $B = 60$. The spectrum is shown for $B \leq 60$ in Fig. 3. Looking at this Figure one can notice two kinds of behaviour. The levels from the first group are the ones which are rapidly, possibly exponentially, convergent to finite energy values and they become constant for large B . These values represent the full non-perturbative eigenspectrum of the “uncut” system. The other curves fall down slowly as

$$E_k(B) \sim \frac{1}{B}. \quad (3.1)$$

These two kinds of curves do not cross but one can see, especially for lower B , that the levels repel each other exchanging their own B -behaviour. For higher B this repulsion is more subtle.

There is a conjecture that the asymptotics of the wave function at large distances, *i.e.* large r , determine the convergence of our calculations being performed with the enlarging number of allowed quanta B [12]. Thus, localized states, whose wave-functions do not go deep into the valleys, converge faster with the cut-off. These states are related to the discrete spectrum of

⁴ To perform the calculation the van Baal’s program [15] was rewritten from Mathematica code to C++. This speeded up the program and made possible computation for higher cut-offs.

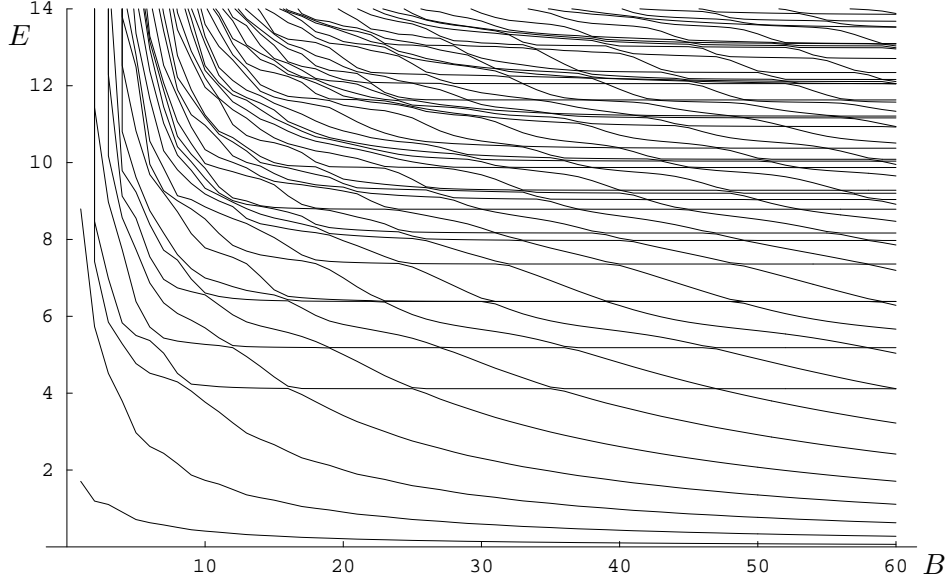


Figure 3. The energy spectrum as a function of cut-off $B \geq n_B$

the Hamiltonian (2.10). They are supersymmetric partners of the localized states from $n_F = 1, 3$ sectors from supersymmetric multiplets [12, 19]. To obtain spectrum of these states the limit

$$E = \lim_{B \rightarrow \infty} E_{B,k} \Big|_{k=\text{const}}, \quad (3.2)$$

is performed where index k enumerates consecutive energy curves and changes only at the anti-crossing points.

On the other hand, the non-localized states penetrate the valleys with increasing the cut-off. They have the power-like behaviour of the energy level. The energy curves which fall slowly to the zero energy with increasing cut-off never converge. They form the continuous spectrum at $B = \infty$. It was in Ref. [18] shown that non-trivial and correct continuum limit for these states is given by

$$E(P) = \lim_{B \rightarrow \infty} E_{B,k(B,P)} \Big|_{P=\text{const}} \quad \text{with} \quad k(B,P) = \frac{P}{\pi} \sqrt{2B} \quad (3.3)$$

where P is the continuous momentum, B is the cut-off and k enumerates only energy levels from the continuous spectrum. The continuous spectrum consists of all positive energy values. Localized and non-localized states coexist as a consequence of the supersymmetric interactions with flat valleys.

It turns out that the vacuum state belongs to the sector with $j = 0$ and $n_F = 2$ and is formed by the continuous spectrum [15, 12]. In order to obtain this state one has to take the states from the continuous spectrum, perform the continuous limit (3.3) and at the end go with $E \rightarrow 0$. Since the SUSY vacuum is constructed from the states with continuous energy spectrum, it is non-normalizable⁵ [12].

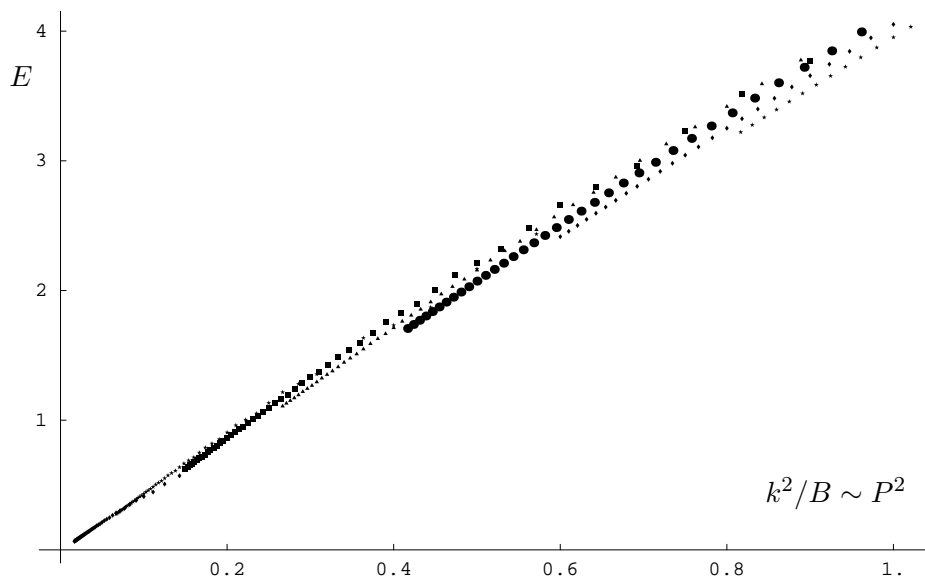


Figure 4. Dispersion relation, $E \sim P^2$, for a few first energy curves from the continuous spectrum. Here, k - enumerates consecutive energy curves for the continuous spectrum and according to [18] k is related to momentum P as $k/\sqrt{B} \sim P$.

3.2. Scaling and dispersion relation

It was shown in Ref. [18] that for the free Hamiltonian the momentum of its eigenstate P is related to a discrete index of consecutive continuous-energy levels k by

$$P \sim \frac{k}{\sqrt{B}}, \quad (3.4)$$

where B is a number of bosons. It turns out that similar dispersion relation holds for our system. This is seen in Fig. 4 where $E(P^2)$ is plotted. In this Figure the energies from a distinct energy curves of continuous spectrum,

⁵ The vacuum state is non-normalizable means its *normalization* to the Dirac delta function.

enumerated by k , are denoted by different symbols. In order to evaluate P Eq. (3.4) was used. Indeed, the points in the plot form a curve $E(P) \sim P^2$ with a very good approximation. Thus, one can suppose that these states form the continuous spectrum at $B = \infty$. This again agree with the continuous nature of scattering states. Therefore, we confirm that the states which correspond to the energy levels with power-like behaviour describe asymptotically free particles. One can imagine that these particles propagate in flat valleys of the potential (2.20).

The above scaling law (3.3) is required to recover the infinite Hilbert space limit (3.3). On the other hand it is interesting because its universality. It is valid for models with only continuous spectrum as well as the mixed one, like the one considered in this work where the Hamiltonians are less trivial and the localized and non-localized states coexist at the same energy.

3.3. Localized versus non-localized eigenfunctions

Applying (2.64) one can also calculate the eigenstates of (2.45). A simple way to analyse the bosonic probability density is to use

$$|\Phi_k(x_1, x_2, x_3)|^2 \equiv \langle \Phi_k(r, u, v) | \Phi_k(r, u, v) \rangle_F, \quad (3.5)$$

where we apply (2.34) while the integration in this product is only performed over the fermionic degrees of freedom.

The energy levels of localized states converge rapidly with B . Similarly, their eigenstates become practically B independent. As one can see due to anti-crossing energy levels (see Fig. 3) the localized states with a specified energy (but considered for different cut-off B) corresponds to distinct values of k . For our convenience we denote the localized states by index (L), *i.e.* $\Phi_s^{(L)}(r, u, v)$, where contrary to $\Phi_k(r, u, v)$ case, index s enumerates only states of the discrete spectrum. A few first bound states are shown in Figs. 5-8. There are mainly localized around the origin where potential has wide minimum – the stadium. These Figures show plots with various cut-off's B . The convergence of the first two states is so good that it is not possible to distinguish the wave-functions with different cut-off's. For higher states with $s = 3$, and $s = 4$ this convergence is worse⁶. This is caused by interference of the states which have nearly the same energy (see Fig. 3). The next state with $s = 5$ is not degenerate and its wave-function also rapidly converges.

In order to observe the symmetry of the localized states we present also contour plot for $|\Phi_s^{(L)}(x_1, x_2, x_3)|^2 = 0.003$ in Figs. 9-10. One can see that

⁶ Because of the simpler shape, the wave-function with $s = 4$ converges more rapidly than one with $s = 3$. However, this convergence is much slower than one for the other wave-functions, *i.e.* with $s = 1, 2, 5, \dots$

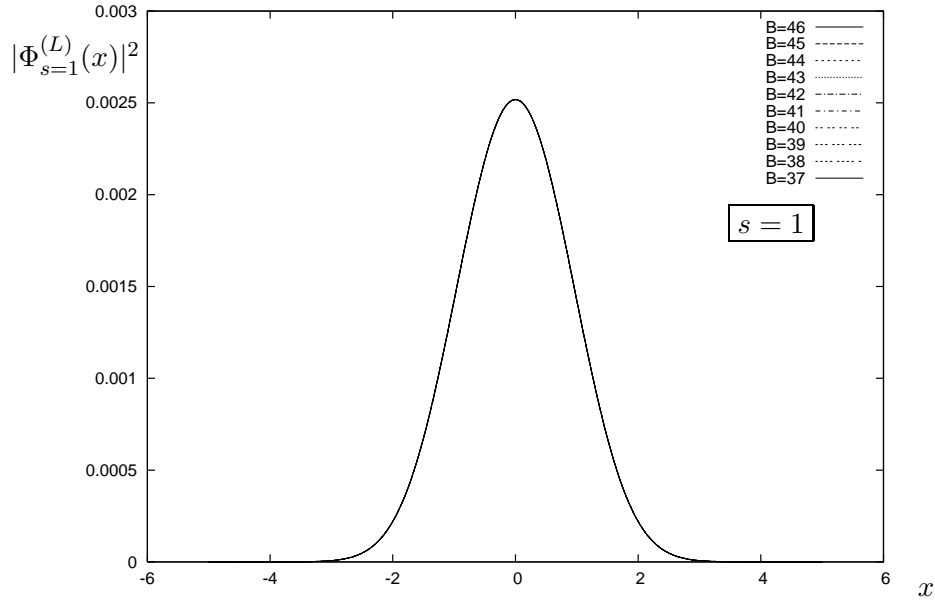


Figure 5. The first bound eigenstate $s = 1$ for $B = 37, \dots, 46$:

$$|\Phi_{s=1}^{(L)}(x, x_2 = 0, x_3 = 0)|^2$$

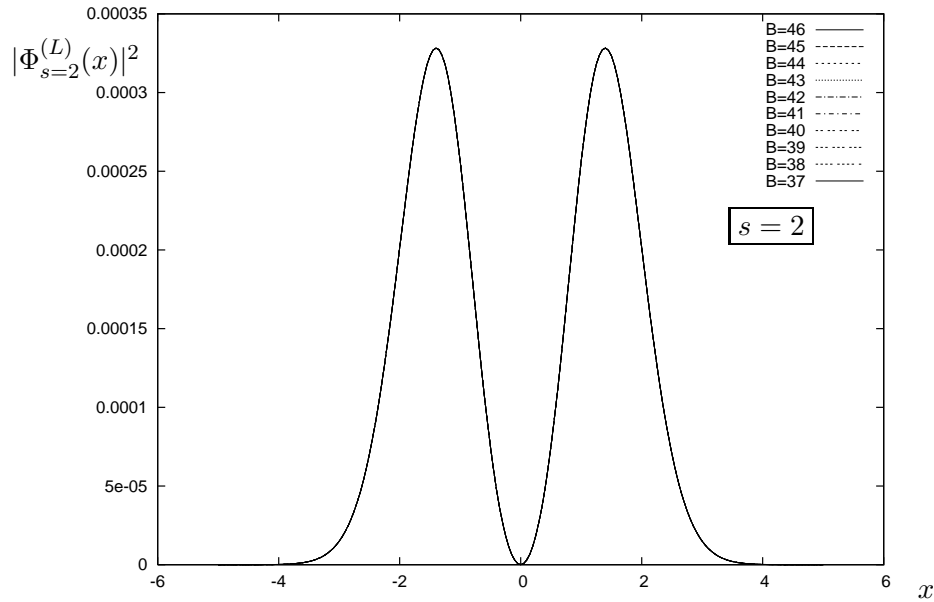
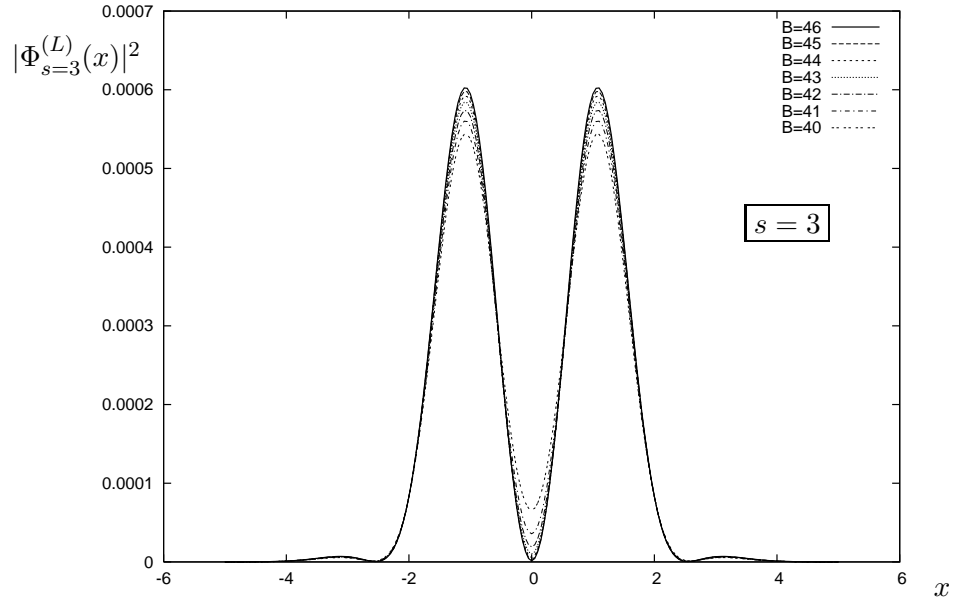
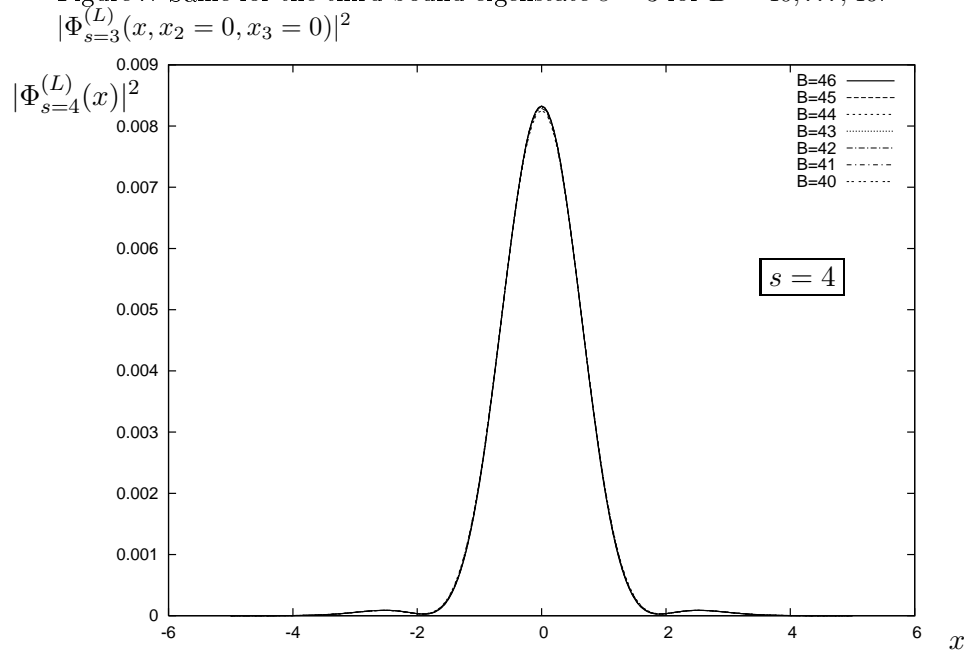


Figure 6. This is Fig. 5 but the bound eigenstate with $s = 2$ for $B = 37, \dots, 46$:

$$|\Phi_{s=2}^{(L)}(x, x_2 = 0, x_3 = 0)|^2$$

Figure 7. Same for the third bound eigenstate $s = 3$ for $B = 40, \dots, 46$:Figure 8. And for the fourth bound eigenstate $s = 4$ for $B = 40, \dots, 46$:

$$|\Phi_{s=4}^{(L)}(x, x_2 = 0, x_3 = 0)|^2$$

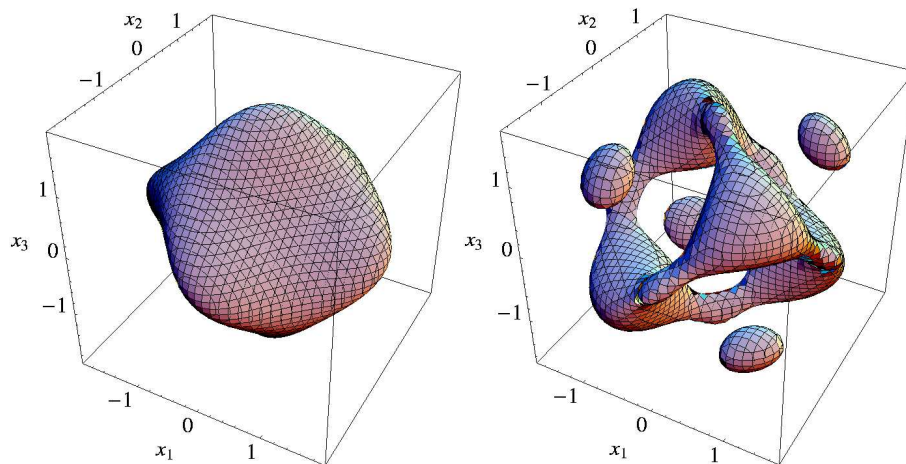


Figure 9. Contour plots for the bound eigenstates with $s = 1, 2$ for $|\Phi_s^{(L)}(x_1, x_2, x_3)|^2 = 0.0003$

only the first bound state possesses the symmetry of the bosonic potential (2.20):

$$x_i \leftrightarrow \pm x_j \quad \text{for } i, j = 1, 2, 3. \quad (3.6)$$

For the remaining states one part of the symmetry (3.6), *i.e.* (2.21), can be broken by the fermionic term in the Hamiltonian (2.33)⁷. Thus, in the fermionic case the symmetry (2.21) is not valid. Although in the considered case $j = 0$ the eigenstates are not spherically symmetric and they have complicated shapes of contour plots with a genus sometimes greater than zero. However, one has to remember that the angular momentum $j = 0$ applies for the 9-dimensional space of \hat{c}_i^a . Since the transformation (2.16) of the \hat{c} -coordinate space to the 3-dimensional x_i -space is non-linear the three-dimensional spherical symmetry in the x_i -space is not obvious.

Let us consider the probability density of states with continuous spectrum along the potential valley:

$$x_1 = x, \quad x_2 = x_3 = 0. \quad (3.7)$$

It turns out that going away from $x_1 = x_2 = x_3 = 0$ the amplitude of the eigenstates (3.5) is strongly suppressed. Thus, to see its dependence along

⁷ H_F contains v variables without square powers. This breaks the symmetry (2.21) of the bosonic potential.

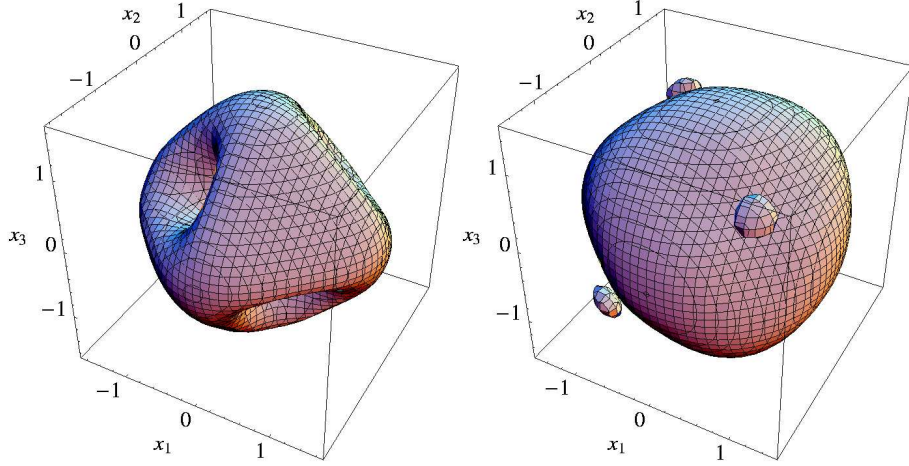


Figure 10. The same contour plots but for the bound eigenstates with $s = 3, 4$ for $|\Phi_s^{(L)}(x_1, x_2, x_3)|^2 = 0.0003$

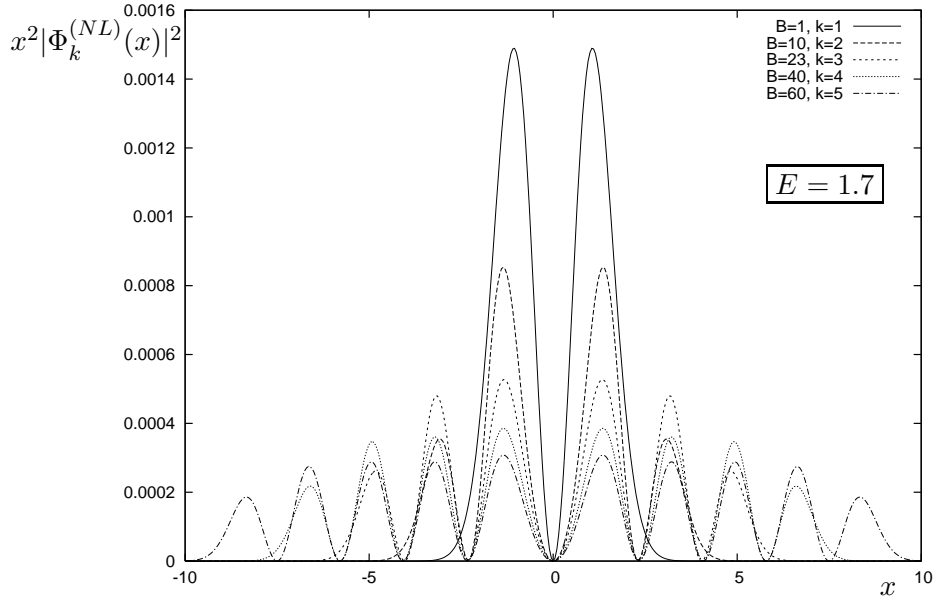


Figure 11. The functions $x^2|\Phi_k^{(NL)}(x)|^2$ for eigenstates with energy levels $E_k(B)$ from the continuous spectrum. Here $E = 1.7$ and $k = 1, 2, 3, 4, 5$.

the valley a quantity

$$x^2|\Phi_k^{(NL)}(x)|^2 \equiv x^2|\Phi_k^{(NL)}(x_1 = x, x_2 = 0, x_3 = 0)|^2 \quad (3.8)$$

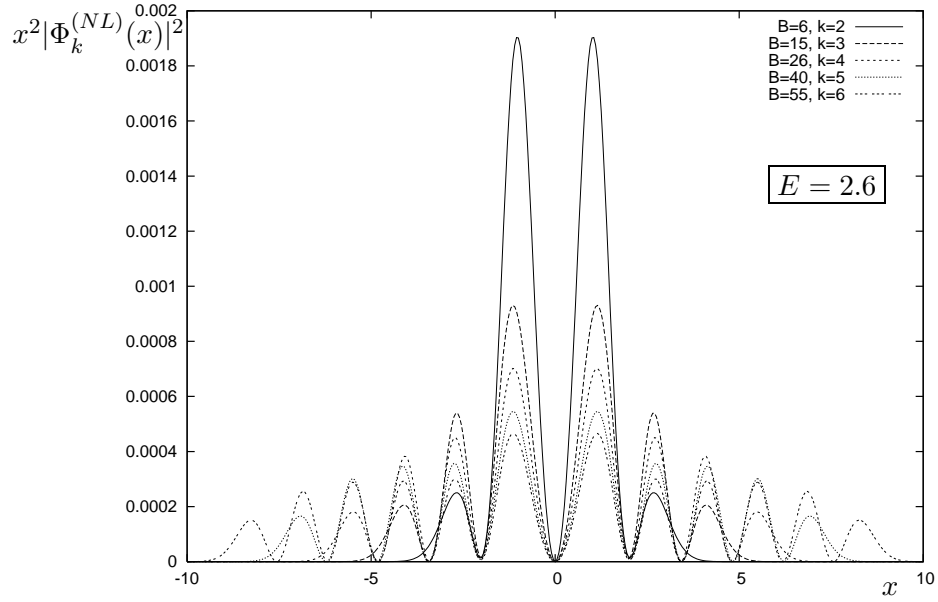


Figure 12. The plot similar to ones from Fig. 11 but for the eigenstates with $E = 2.6$ and $k = 1, 2, 3, 4, 5$.

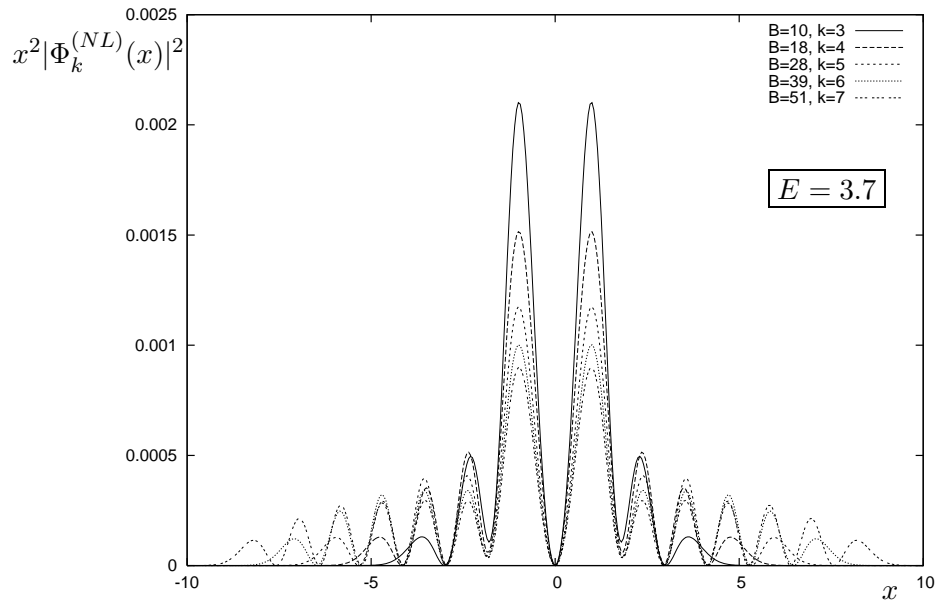


Figure 13. The same function as in Fig. 11 but for $E = 3.7$ and $k = 1, 2, 3, 4, 5$.

is studied. Similarly to the localized states the non-localized ones are denoted by superscript (NL) , *i.e.* $\Phi_k^{(NL)}(x_1, x_2, x_3)$, and their index k enumerates only the energy levels from the continuous spectrum. The scaling limit implied in (3.3) is performed as follows. Take an arbitrary energy, *i.e.* $E = 1.7$, and for a given energy curve from the continuous spectrum, *i.e.* $E_k^{(NL)}(B)$ enumerated by index k , find the cut-off B which best satisfies the following condition

$$E_k^{(NL)}(B) = E, \quad (3.9)$$

where E is the arbitrary energy. The probability density of the Hamiltonian eigenstates multiplied by x^2 (3.8) is shown for $E = 1.7$ and $k = 1, 2, 3, 4, 5$ in Fig. 11. As one can see for $k = 1$ the function $x^2|\Phi_k^{(NL)}(x)|^2$ has two peaks. For the next energy curve, *i.e.* $k = 2$, the plot has four peaks with lower amplitudes. Thus for the k -th curve one can see $2k$ peaks. In the limit (3.3) the amplitudes of the peaks for a given energy are nearly the same. This does not occur for the peaks in the centre of the potential and the peaks deeper sunk in the valley. For all k the oscillations of frequencies are nearly the same and correspond to the energy $E = 1.7$. For higher energies, *i.e.* $E = 2.6$ and $E = 3.7$ presented in Fig. 12 and Fig. 13 respectively, frequencies are lower but for the fixed energy value they are approximately independent of k . Taking states for higher energy curves one can notice that their wave-functions enter deeper into the valleys (2.20). This fact confirms that the considered states form the continuous spectrum for $B \rightarrow \infty$.

In the purely bosonic sector, *i.e.* where $n_F = 0, 6$, as well as in the sectors with $n_F = 1, 5$, where bosonic modes are dominating, despite the flatness of the potential valleys the flat directions are blocked by the energies of the transverse quantum fluctuations. This makes the spectrum in zero-fermion and one-fermion sectors discrete. However, in the supersymmetric system the transverse fluctuations cancel among bosonic and fermionic states. Thus, valleys are not blocked and in the model with supersymmetric fermions the continuous spectrum appears. This occurs in sectors for $n_F = 2, 3, 4$.

On the other hand, we have sectors with only discrete spectra, *i.e.* $n_F = 0, 1, 5, 6$. The supersymmetry creates super-multiplets and demands the existence of similar states in others sectors. Therefore in the central sectors, *i.e.* $n_F = 2, 3, 4$, there is coexistence of discrete and continuous spectra. This is exactly what Fig. 3 shows.

4. Summary

Despite the fact that Supersymmetric Yang-Mills Quantum Mechanics (SYMQM) models [1, 2] are simpler than the original field theories, they still pose difficult to solve complex problems. On the other hand we have the

BFSS equivalence hypothesis [3, 4, 5], which relates SYMQM to M -theory. This makes SYMQM even more interesting. Moreover, the SYMQM models form very good laboratory for learning of supersymmetric theories. Studies in their zero-fermion sectors, *i.e.* of the non-supersymmetric Yang-Mills mechanics, give us knowledge about 0-volume glueball states, [9, 10, 11, 12]. On the other hand testing relations between fermionic sectors we can observe specific properties of the action of the supersymmetric operator.

In this work we have considered the $D = 4$ dimensional model with $SU(2)$ gauge groups. This model is non-trivial and possesses both localized and non-localized states. There were many approaches [12, 13, 15, 19] to understand the model and to find its energy spectrum. We have followed the method [15] proposed by van Baal which allows to solve problem in the sector with specified not only the number of fermionic quanta n_F but also at the fixed momentum $j = 0$. We have chosen the sector with $n_F = 2$ and $j = 0$, where the supersymmetric vacuum should appear.

First, the energy spectrum for very high cut-offs $B \leq 60$ has been calculated. It exhibits complex structure of the states, *i.e.* coexistence of localized and non-localized states. For a high cut-offs, *i.e.* $B > 40$, not only the energies of localized states become B -independent but also the corresponding eigenfunctions. We have constructed the first few bound state and described their properties. Our spectrum agree with the previous results [12, 13, 15, 19]. However, with the higher cut-off it is much more accurate.

In the plot of the energy spectrum as a function of the cut-off B in Fig. 3 the non-localized states form curves behaving as $1/B$. Taking the states from these curves for a constant energy we have studied the properties of the eigenfunction from the continuous spectrum. At the end we have tested the scaling of the continuous spectrum (3.3) and confirmed numerically dispersion relation of the free particles presented in Ref. [11]. The scaling was derived in Ref. [18] for models with only non-localized states whereas here we have shown that with a very good approximation is also valid for the non-trivial interactions.

5. Acknowledgements

I thank Jacek Wosiek for suggesting the subject and fruitful discussions and Pierre van Baal for making the program for calculation the energy spectrum available for me. I also acknowledge discussions with Maciej Trzetrzelewski. This work was supported by the grant of the Polish Ministry of Science and Education P03B 024 27 (2004-2007).

References

- [1] E. Witten. Dynamical breaking of supersymmetry. *Nucl. Phys.*, B188:513, 1981.
- [2] M. Claudson and M. B. Halpern. Supersymmetric ground state wave functions. *Nucl. Phys.*, B250:689, 1985.
- [3] T. Banks, W. Fischler, S. H. Shenker, and L. Susskind. M theory as a matrix model: A conjecture. *Phys. Rev.*, D55:5112–5128, 1997.
- [4] D. Bigatti and Leonard Susskind. Review of matrix theory. 1997. hep-th/9712072.
- [5] W. Taylor. M(atr)ix theory: Matrix quantum mechanics as a fundamental theory. *Rev. Mod. Phys.*, 73:419–462, 2001.
- [6] M. Dine, R. Echols, and J. P. Gray. Tree level supergravity and the matrix model. *Nucl. Phys.*, B564:225–240, 2000.
- [7] J. Polchinski. String theory. Cambridge, UK: Univ. Pr. (1998).
- [8] M. B. Halpern and C. Schwartz. Asymptotic search for ground states of su(2) matrix theory. *Int. J. Mod. Phys.*, A13:4367–4408, 1998.
- [9] M. Luscher. Some analytic results concerning the mass spectrum of yang-mills gauge theories on a torus. *Nucl. Phys.*, B219:233–261, 1983.
- [10] M. Luscher and G. Munster. Weak coupling expansion of the low lying energy values in the su(2) gauge theory on a torus. *Nucl. Phys.*, B232:445, 1984.
- [11] P. van Baal. Gauge theory in a finite volume. *Acta Phys. Polon.*, B20:295–312, 1989.
- [12] J. Wosiek. Spectra of supersymmetric yang-mills quantum mechanics. *Nucl. Phys.*, B644:85–112, 2002.
- [13] J. Kotanski and J. Wosiek. Hamiltonian study of supersymmetric Yang-Mills quantum mechanics. *Nucl. Phys. Proc. Suppl.*, 119:932–934, 2003.
- [14] Jeffrey Koller and P. van Baal. A nonperturbative analysis in finite volume gauge theory. *Nucl. Phys.*, B302:1, 1988.
- [15] P. van Baal. The Witten index beyond the adiabatic approximation. 2001. To appear in the Michael Marinov Memorial Volume, 'Multiple Facets of Quantization and Supersymmetry', edited by M. Olshanetsky and A Vainshtein, World Scientific.; hep-th/0112072; www.lorentz.leidenuniv.nl/vanbaal/susyYM.
- [16] B. de Wit, M. Luscher, and H. Nicolai. The supermembrane is unstable. *Nucl. Phys.*, B320:135, 1989.
- [17] H. Nicolai and R. Helling. Supermembranes and m(atr)ix theory. 1998. hep-th/9809103.
- [18] M. Trzetrzelewski and J. Wosiek. Quantum systems in a cut Fock space. *Acta Phys. Polon.*, B35:1615–1624, 2004.
- [19] M. Campostrini and J. Wosiek. High precision study of the structure of $D = 4$ supersymmetric Yang-Mills quantum mechanics. *Nucl. Phys.*, B703:454–498, 2004.